Characterizing WiFi Link Performance in Open Outdoor Networks

Utpal Paul
Computer Science Department
Stony Brook University
upaul@cs.sunysb.edu

Riccardo Crepaldi
Computer Science Department
University of Illinois at Urbana-Champaign
rcrepal2@illinois.edu

Jeongkeun Lee, Sung-Ju Lee, Raul Etkin
Hewlett-Packard Laboratories
Palo Alto, CA
{jklee, sjlee, raul.etkin}@hp.com

***Abstract*—We present an experimental performance evaluation study of WiFi links in an open-space outdoor environment. We consider a large scale wireless sensor network scenario of seismic data collection from sensors that are buried in ground and a set of access points (APs) form the hierarchical aggregation layer and the backbone of the network. We conduct two different link characterization studies. First, we evaluate the links between the sensor nodes and a wireless AP using IEEE 802.11a/b/g. We construct the path loss model and investigate the reachability distance of this link for different protocols and different sensor node antenna heights. We then characterize the long distance wireless backhaul links between the APs. We use 802.11n and high gain directional antenna for high throughput and long distance. We evaluate how different PHY and MAC layer enhancements of 802.11n impacts its performance in an open outdoor environment. We observed up to 148 Mb/s throughput at 800 meter line-of-sight links without sophisticated tuning of antenna orientation. We believe our findings can be a benchmark for WiFi based outdoor network deployment, especially for high throughput long distance links.**

I. Introduction

WiFi-based long distance networks have become very popular in providing Internet access to the remote areas in developing regions [22], [25]. The unlicensed WiFi spectrum and a variety of commodity IEEE 802.11 hardware make WiFi an attractive communication method because of its wide availability and low cost. These networks typically have long distance point-to-point wireless links enabled by high-gain directional antennas where the links are typically several kilometers long, but often provide low throughput. Their long distance wireless links usually require permanent structures as the antennas are placed on top of a tower or a tall building. Moreover, fine-grain tuning of antenna orientation is needed to achieve the maximum gain (up to 24 dB) having narrow beam widths (down to 8 degrees).

We consider a network in an open space outdoor environment with a different scenario where a large number (millions) of sensors are deployed to collect seismic data covering a huge geographic space for the purpose of oil and gas exploration [11]. The sensor data needs to be collected and delivered to a centralized command unit. The network must run on unlicensed bands for its wide deployability and hence we use a WiFi based solution. As our network is large in scale of both the number of nodes and area to cover, we build a hierarchical network. A very abstract level design of our network architecture is shown in Figure 1. In our scenario, the sensors are buried in the ground to accurately capture the seismic data. Each Access Point (AP) covers a space where the sensors in that space communicate to that AP. A set of APs forms the aggregation layer or the backhaul. The APs of one aggregation layer communicates to an AP of the next higher layer, and vice versa. As this deployment is not permanent and needs to be moved to collect data in other area, it is not desirable to setup a permanent structure to mount the APs. In our scenario, the APs are mounted on top of a light-weight movable mast that may be $4 \sim 5$m tall. A similar hierarchical sensor network architecture has been deployed to monitor real-world habitats [20].

We characterize the WiFi link performance of the network under consideration. First, we study the first hop link, that is, the link between a sensor node and an AP. For this link, high throughput is not required, but the link range is an important concern from the perspective of network design. We consider 802.11a/b/g for this link. [1] For a backhaul link between two APs, high throughput as well as distance are required as it transmits the aggregated data from a large number of sensors towards a remote data collection & command center. We consider 802.11n for this link because the 802.11n MIMO (Multiple Input Multiple Output) technique and MAC enhancements provide high throughput without requiring stronger signal power than 802.11a/g. Thus, narrow-beam high gain directional antennas and sophisticated orientation settings are not needed. We instead use *polarized* directional MIMO antenna with nominal gain (13.5 dB) to generate enough path orthogonality for MIMO operations even with Line-of-Sight (LOS) links in an open environment, where rich scattering and multipath might not be available.

Our contributions are the following:

- We study how different modulation schemes (Differential Binary Phase Shift Keying 1 Mb/s vs. Orthogonal Frequency Division Multiplexing 6 Mb/s), center frequency (2.4 GHz vs. 5 GHz) and antenna heights at the sensor nodes affect the maximum communication distance.
- We evaluate the performance of 802.11n in an open

[1] 802.11n may provide better link range with diversity gain. Because of the simplistic design of the sensor node, it is not possible to use multiple antennas at the sensor node. Thus, there is no link range benefit by using 802.11n for this link.

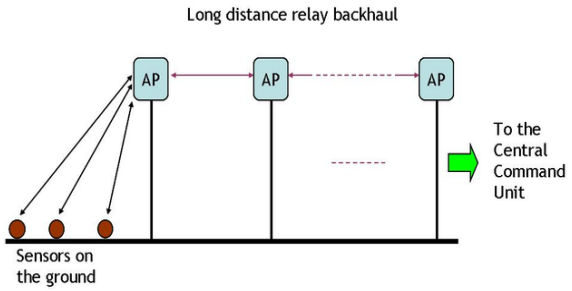

Fig. 1. A conceptual diagram of our network architecture.

outdoor environment. 802.11n MIMO utilizes multi-path effect and is well suited for indoors or urban environments. We show 802.11n is still effective in a desert-like open environment.

- We analyze how several PHY/MAC enhancements of 802.11n improve the performance in an outdoor network. We discover that the enhancements enable 802.11 to be effective in outdoor networks as in indoor networks.
- We reveal that in our experiments, throughput degradation in longer distance links results from reduced received signal strength and not from decreasing diversity gains. Two MIMO streams are well supported up to our longest link of 1800 meters, by the dual-polarization patch antenna with two vertically and one horizontally polarized antenna elements. With the robust Modulation and Coding Schemes (MCS), even three MIMO streams are sustained.

The rest of the paper is organized as follows. We discuss related work in Section II and present our experimental results from the sensor-to-AP links in Section III. Characterization of backhaul links using 802.11n is presented in Section IV. We conclude in Section V.

II. RELATED WORK

There is a large amount of work on long distance WiFi in outdoor networks. Raman *et al.* [13] are among the first to deploy a WiFi based outdoor long distance network consisting of approximately ten links and lengths ranging from 1∼16 Km. In [14], a systematic study of long distance 802.11b link performance is performed. They study the behavior of such long links for varying packet sizes, data rates, SNRs and weather conditions. They also present a modification to the MAC protocol for long distance mesh networks [25]. The authors in [17] present a measurement study of outdoor 802.11g links. Sheth *et al.* [28] present a study on most common sources of packet losses in long distance links. In [22], Patra *et al.* present a modification to the MAC protocol and design a TDMA based MAC protocol which is more robust in lossy conditions for long distance links. There is a basic difference between these work and our scenario under consideration. All these work have infrastructured APs on top of towers or high buildings to create LOS links. In addition, their main focus is to provide network connection over long-distance (up to 16 Km) point-to-point link and high throughput is not their major concern. In contrast, our network requires high bandwidth and has relaying APs every 1∼2 Km. We evaluate 802.11n for long distance links in a rural environment where there is less multipath effect than indoor and urban environments.

Shrivastava *et al.* [29] present the first experimental study of 802.11n and quantify different mechanisms introduced in 802.11n in diverse conditions. They show that the throughput of an 802.11n link can be severely degraded in presence of an 802.11g link. Pelechrinis *et al.* [24] evaluate the packet delivery ratio of an 802.11n link when operating at the high transmission rates supported by 802.11n. They show that these high transmission rates typically produce losses, even in absence of interference due to the lack of rich multipath even in indoor environments. In our experiments, we observe that polarization antenna provides enough diversity gain for the links of up to 1800 meters for MCS indices of two streams. The highest achievable throughput of a lossless 802.11n link in an indoor testbed for each PHY/MAC layer enhancements offered by 802.11n is reported in [23]. We also evaluate the performance gain achieved for different enhancements and show that our results obtained in an outdoor network are comparable to their findings. Arslan *et al.* [12] present an auto-configuration framework for enterprise 802.11n WLAN that integrates channel bonding and user association. Gelal *et al.* [15] present an in depth study to show the impact of MIMO diversity on higher layers. All these studies on 802.11n are performed in indoor testbeds. The authors in [16] present a theoretical model of outdoor MIMO channel in a LOS environment. They show that, in a pure LOS situation, path orthogonality can only be achieved for very short distance links when the conventional linear array antenna model is used with no polarization diversity.

The gain of polarization antenna diversity on MIMO channel with LOS components has been studied and reported in [18], [27], [21]. However, their measurement experiments are performed in small indoor environments or even more controlled anechoic chambers using custom tailored antenna and devices because their main focus was to validate their theoretical models by measurements. To our best knowledge, our paper is the first measurement report that shows the polarization diversity gain for long distance outdoor communication using commodity 802.11n devices.

III. SENSOR-TO-AP LINK

In this section, we characterize the fist hop link, that is, the link from the sensor node to the AP node. We present results of Received Signal Strength (RSS) and throughput measurements to characterize the effect of antenna height and frequency band (i.e. 2.4 GHz or 5 GHz) on reachability. In addition, we use our measurements to fit parameters of a simple path loss model. We start with a detailed description of our experimental setup and then present our analysis.

A. Experimental Setup

For experiments here and in Section IV, the challenge was to find locations with open, flat space that has no wireless or

Fig. 2. Set up of a WCB node on the ground.

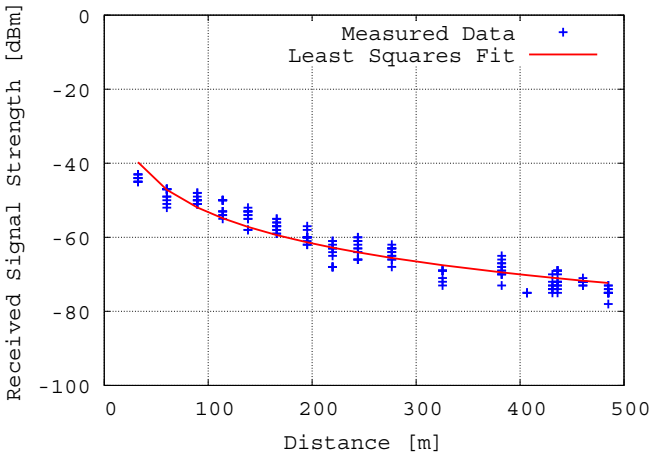

Fig. 3. Measured received signal strength and least squares fit of the data using WCB height of 1 meter as a function of transmitter-receiver distance.

human interference. This experiment is performed in a walking trail in the Baylands Preserve in Palo Alto, California, USA. The trail is straight, flat, and has a length of about 550 m. There are no major obstacles in the trail, ensuring complete line of sight between the transceivers' antennas when there is no moving person or object in the trail.[2]

We use an HP E-M111 Wireless Client Bridge (WCB) [4] acting as a sensor node and an HP E-MSM422 AP [5]. The AP is kept fixed at one end of the trail and is connected to an external antenna with omni-directional horizontal radiation pattern and 12 dBi of gain (Laird Technologies OD24-12 [8] for 2.4 GHz band and Laird Technologies OD58-12 [9] for the 5.4-5.8 GHz band). The antenna is mounted on top of a tripod that is 3 m high.

The WCB has an external dipole antenna with 2 dBi gain and omni-directional horizontal radiation pattern. Figure 2 shows the complete set up of a WCB node. We position the WCB at different locations to create different link lengths. Considering our application scenario, this link does not require high throughput. However, higher throughput results in shorter transmission times which in turn may allow for energy savings. Nevertheless, reachability of the link, that is, maximum communication distance without significant packet losses, is our main interest. We use 802.11a/b/g for our experiment to investigate how reachability varies for different frequency bands and modulation schemes.

In our oil and gas exploration scenario, the sensor nodes are buried in the ground to capture the seismic data, but we can have a tethered node design to have the antennas above the ground. To evaluate the impact of the height of the sensor node's antenna on the link reachability, we place the WCB at four different height levels. The height levels are: Level 0 (on the ground), Level 1 (10 cm above the ground), Level 2 (50 cm above the ground) and Level 3 (1 m above the ground).

The wireless devices are configured to channel 1 of the 2.4GHz band for 802.11b and g, and channel 149 of the 5GHz band for 802.11a. We set the transmission power to the maximum supported by each device, that is, 20 dBm for the WCB, and 18 dBm for the AP. Both the AP and the WCB are powered by battery and are connected to laptops using the ethernet cable. We run iperf [7] to create UDP flows between the two laptops connected to the two wireless devices. Each iperf session lasts for 60 sec. For each measurement run, we record the throughput and the RSS at both ends of the link using SNMP (Simple Network Management Protocol) commands.

[2]There were bicycles and joggers passing the trail occasionally and we paused the experiments in cases where the moving objects block the line-of-sight link. However, we were not able to completely remove the effect of moving objects and they might have caused some level of signal strength variation.

B. Experimental Results

First, we use RSS measurements to fit parameters of a simple path loss model. Theoretical and measurement-based propagation models indicate that the average received signal power decreases logarithmically with distance [26]. Therefore, we use

$$P_r = K \cdot P_t / d^{\alpha} \tag{1}$$

to model the received signal power P_r for a given transmit signal power P_t, and transmitter-receiver distance d [26]. In (1), α is called the path loss exponent, and takes values between 2 and 6 depending on the propagation environment. K is a constant that depends on the transmission frequency, antenna gains, and antenna heights. In dB scale (1) takes the form

$$P_r[\text{dBm}] = P_t[\text{dBm}] + K[\text{dB}] - 10\alpha \log_{10} d$$

which exhibits a linear dependence between the received signal power in dB and the logarithm of the transmitter-receiver distance.

Figure 3 shows 180 received signal strength (RSS) measurements when the nodes are configured for 802.11b for different link lengths with a WCB height of 1 m. It also shows the least squares fit of the measured data using (1) optimizing over K and α. Similar least squares fits were performed for other WCB heights, which are shown in Figure 4. The corresponding

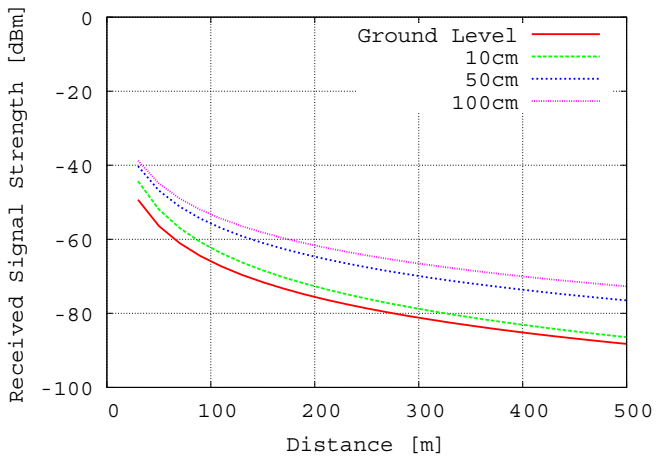

Fig. 4. Received signal strength (least squares fit of measurements) as a function of transmitter-receiver distance for different WCB heights.

TABLE I
OPTIMAL PARAMETERS

WCB height	K [dB]	path loss exponent α
0 m	-22.26	3.19
10 cm	-13.31	3.45
50 cm	-16.43	2.97
1 m	-17.71	2.78

values of K and α resulting from the least squares fit of the measured data are shown in Table I.

Referring to Table I, we observe the following trend for WCB heights ranging from 10 cm to 1 m: taller heights result in a reduction of K and α. We believe the increase of K with lower WCB heights is due to the interaction of the WCB antenna and the ground. We conjecture that placing the WCB closer to the ground may slightly modify the radiation pattern of the antenna, increasing its effective gain. In addition, larger WCB heights reduce the detrimental effects of the component of the signal that is reflected on the ground, resulting in a smaller path loss exponent α.

These trends, however, are not followed by the measurement results with the WCB placed on the ground. Table I shows a reduction in K of 8.95 dB resulting from reducing the WCB height from 10 cm to 0 cm. We conjecture that placing the WCB antenna so close to the ground affects the radiation characteristics of the antenna, possibly modifying its gain and impedance. For future work, it may be fruitful to investigate other antenna designs, for example based on a monopole with a ground plane, that may be less affected by being placed close to the ground.

The measurements with the WCB on the ground also exhibited more variability, that is, the squared error of the fit was larger than in the other cases. With the WCB on the ground, small irregularities in the terrain, small vegetation or obstructions such as little rocks may create obstructions and attenuate the signals. Therefore, increasing the WCB height not only improves the mean RSS, but also makes the link more reliable.

We next investigate the link reachability for different 802.11 protocols and WCB heights. We tested reachability by reducing the distance between AP and WCB until the association is stable and does not break within a short period of time. After association, we continued reducing the distance until obtaining at least 50% successful receiption of ping replies for 10 seconds. Figure 5 shows the longest link range possible for 802.11a/b/g, each operating at the lowest possible physical data rate (i.e. OFDM 6 Mb/s for 802.11a/g and DBPSK 1 Mb/s for 802.11b).

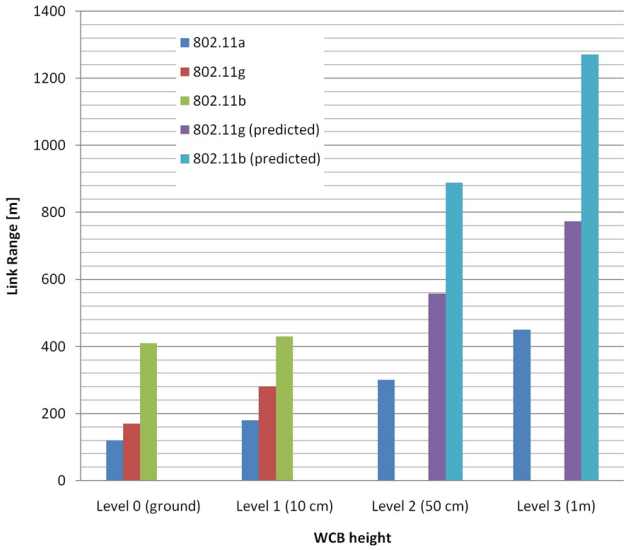

Fig. 5. Link reachability for different 802.11 protocols for different height levels of WCB.

We note that the measurement results for 802.11b/g with WCB height of 0.5 and 1 m were limited by the length of the field where we performed the test. As a result,we represented the corresponding values using predictions derived from our model as follows. The reachability of 802.11g for WCB height of 10 cm is 280 m, and the corresponding RSS derived from the least squares fit of the data is -78 dBm. To estimate the reachability for WCB heights of 50 cm and 1 m, we use our model and estimated parameters to find the distance at which the RSS is -78 dBm. The corresponding estimated reachability distances for 802.11g are 558 m and 773 m. Similarly, we observe that the reachability of 802.11b for WCB height of 10 cm is 430 m, and the corresponding least squares fit of the RSS data is -84 dBm. For WCB heights of 50 cm and 1 m, our model predicts this RSS at distances of 888 m and 1270 m, which should be the corresponding reachability distances.

We see that antenna height plays an important role in link distance. In addition, the use of lower frequencies (11g 2.4 GHz over 11a 5 Ghz while the same modulation) and lower data rates and more robust modulation schemes (11b 1 Mb/s over 11g 6 Mb/s in the same frequency), all contribute to increasing the communication range.

IV. AP-TO-AP BACKHAUL LINK

Backhaul links carry the aggregated data from the sensor nodes. This demands high throughput links for the backhaul and we use 802.11n. We briefly describe key PHY/MAC

enhancements of 802.11n and evaluate how they impact the throughput of long distance outdoor links.

A. Background

802.11n uses different PHY and MAC layer mechanisms to achieve high throughput. We review some of these features.

1) Frame Aggregation and Block Acknowledgement: In order to reduce the MAC overhead, 802.11n allows grouping multiple consecutive frames to form an aggregate frame. Frame aggregation hence increases the utilization of each channel access. One type of aggregation is A-MPDU (Aggregated MAC Protocol Data Unit) where multiple MAC frames (MPDUs) are combined. On the other hand, multiple upper layer packets coming to the MAC layer is aggregated to form A-MSDU (Aggregated MAC Service Data Unit).

In legacy MAC protocols, an ACK frame is always sent by the receiver for each correctly received data frame. 802.11n allows the receiver to send a single acknowledgement frame, called Block-Acknowledgement for several received frames. This also reduces the MAC layer overhead. An A-MPDU frame has CRC for its each subframe (MPDU) and the use of Block-ACK and A-MPDU enables the retransmission of corrupted subframes only instead of the entire aggregate frame, which is the case of A-MSDU. Thus, A-MPDU has additional MAC frame overhead for each subframe but it has lower retransmission cost compared to A-MSDU. We test A-MPDU in our experiments.

2) Channel Bonding: 802.11n introduces channel bonding where two adjacent channels are bonded to have a wider channel. Legacy 802.11 mode only supports 20MHz channels while the 802.11n specification allows the use of 40MHz bonded channels, which doubles PHY data rates. However, when using a wider channel, there are fewer channels available for use by other 2.4GHz or 5GHz devices. Moreover, the use of wider channels is more prone to interference and reduces received power at the receiver by 3 dB because the transmitted energy spreads over twice the channel width.

3) Guard Interval: An additional technique used to improve the throughput in 802.11n transmissions is to shorten the guard interval. The guard interval is a time interval inserted between orthogonal frequency division multiplexing (OFDM) symbols in which no valid data is transmitted. The purpose of this guard interval is to reduce intersymbol and intercarrier interference. The 802.11n specification allows for a reduction of this guard interval from 800 ns (defined in the 802.11a and 802.11g specifications), referred as Long Guard Interval (LGI), to 400 ns, referread as Short Guard Interval (SGI). Theoretically SGI provides 11% increase in PHY data rate [6].

4) PHY Layer Diversity: In addition to the MAC layer mechanisms, 802.11n uses different physical layer enhancement techniques to improve performance. 802.11n uses MIMO antennas with spatial diversity and spatial multiplexing. In the transmitter side, this can be achieved using SDM (Spatial Division Multiplexing) and STBC (Space Time Block Coding). In SDM, multiple independent fading signal paths are used to reduce error probability. These multiple streams

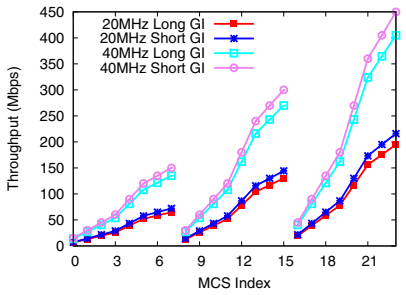

Fig. 6. PHY layer data rates provided by each MCS index for each combination of channel width and guard interval. MCS 0 to 7 indicate one data stream, MCS 8 to 15 indicate two data streams whereas MCS 16 to 23 indicate three data streams.

are multiplexed using multiple antennas spaced sufficiently apart by half of the wave length. STBC is a pre-transmission encoding done by a MIMO transmitter that allows it to improve the signal-to-noise ratio even at a single RF receiver. Receiver side diversity gain is achieved by using Maximal Ratio Combining (MRC), that exploits spatial diversity. In MRC, a weighted sum of signals received on all antennas, taking into account the SNR of each receive antenna, results in the combined signal being stronger than the signal received with maximum power.

Various modulation and coding schemes are defined by the 802.11n spec [6], and are represented by a Modulation and Coding Scheme (MCS) index value. Figure 6 shows the PHY rates at different MCS indices for each combination of channel width and guard interval as defined in the spec. Note that MAC and application throughput will be less than the the specified PHY data rates mainly due to the MAC layer overhead including backoff and retransmissions caused by packet losses. The spec defines MCS indices up to four MIMO streams but we only plot one to three stream MCS indices in Figure 6, as we use 802.11n chipset from Atheros that supports up to 3×3 MIMO streams.

B. Experimental Setup

We perform the backhaul experiments in an open space flat land that is the property of UC Davis Department of Plant Sciences. We selected this location as it provides a line-of-sight link of up to 1.8km with very little obstruction. Moreover, we did not detect any wireless interference on the 5 GHz band where we do the measurements. Figure 7 shows the satellite view of this location. We characterize the backhaul link for different link lengths: 300m, 800m and 1800m. One end of the link is fixed and we move the other end of the link to generate different link distances.

The wireless nodes used in our experiment are reference boards using the wireless card based on Atheros AR9380 chipset [2]. This card supports 3×3 MIMO operation and have three antenna connectors. It supports both 2.4GHz and 5GHz bands, and channel widths of both 20MHz and 40MHz. We use Atheros proprietary driver software to configure the reference board for our experiments. The driver allows us to change the options for channel width, guard interval and frame

Fig. 7. Satellite view of the location where the experiment for the backhaul link testing is conducted. Node locations are shown using circles. The green node is kept fixed while the second node is moved to other locations to generate different link lengths.

Fig. 8. Antenna setup at one end of the link.

aggregation. Each wireless node is connected to a 3×3 MIMO antenna where two of the antenna elements are vertically polarized and one is horizontally polarized [1]. This MIMO antenna has a 13.5 dBi gain and 20 degree beamwidth at 5.5 GHz. All three connectors of the antenna are connected to the radio. The antennas are mounted on top of tripods that are 3m high. We use SDM mode as it generates higher capacity than STBC mode.

We constructed a WDS (Wireless Distributed Links) link between the two wireless nodes where one is configured as the Master node, while the other one as the client node. We configure the nodes to operate on channel 149 of the 5 GHz band. We disable the card's automatic rate adaptation scheme and manually set a fixed MCS for each experiment. We use the maximum transmit power of the chipset all throughout the experiments. We use different channel widths and vary MCS rates. Each wireless node is connected to a laptop using the ethernet cable. We use iperf [7] to generate UDP flows with

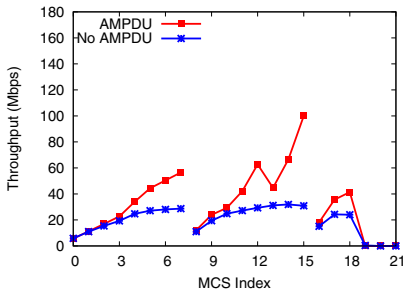

(a) 20MHz channel width and long GI

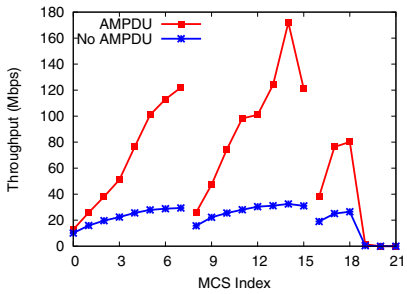

(b) 40 MHz channel width and short GI

Fig. 9. Throughput for 300m link lengths

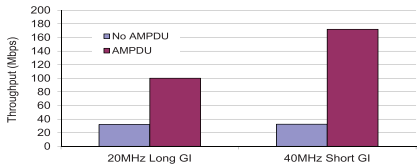

Fig. 10. Throughput improvement for frame aggregation for 300m link.

default packet size of 1470 bytes between the two laptops. Figure 8 shows the setup at one end of the link.

As also pointed out in [14], MAC layer ACK timeout value is an important parameter in long-distance link tests. As the distance increases, propagation delay increases and the use of short timeout for long distance links can result in significant throughput degradation due to unnecessary frame retransmissions. The default timeout in the driver is 24μs and we used it for the 300 meter link. For 800 and 1800 meter experiments, we increase it to 38μs to avoid false ACK timeouts.

C. Measurement Results

1) Frame Aggregation: We first analyze the performance gain from frame aggregation. Figure 9 shows the throughput of the 300m link when the link is configured for a) 20MHz channel width, long guard interval and b) 40MHz channel width, short guard interval. The plot shows the throughput achieved from both enabling and disabling frame aggregation. Note that we could not establish link connectivity for the high MCS rates (MCS index greater than 18). The plot indicates a huge improvement of throughput with frame aggregation relative to without frame aggregation. This is expected as frame aggregation reduces the MAC layer overhead. We plot

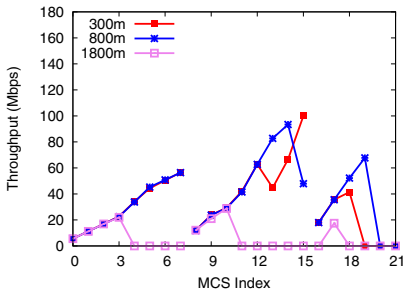

(a) 20MHz channel width

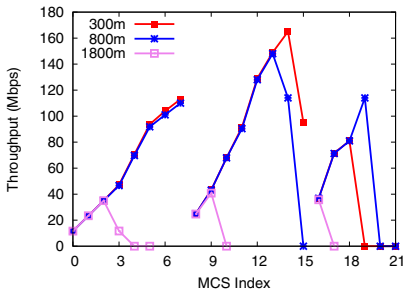

(b) 40 MHz channel width

Fig. 11. Throughput for different link lengths with frame aggregation and long GI.

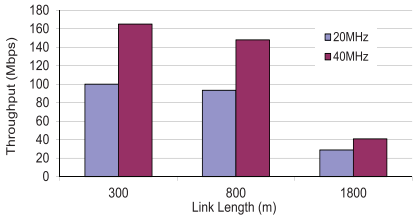

Fig. 12. Throughput improvement for channel bonding for different link lengths. Frame aggregation is enabled and long GI is used.

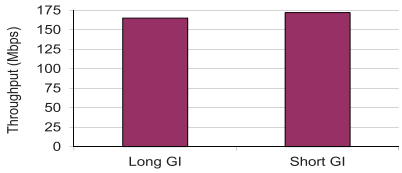

Fig. 13. Throughput improvement by using short guard interval for 300m link with frame aggregation enabled.

the maximum throughput achieved in each configuration for this link in Figure 10. We see that with the configuration of 20MHz channel width and LGI, there is more than 200% throughput improvement from frame aggregation. In addition, we see 450% throughput improvement for 40MHz channel width and SGI. This is higher than the throughput improvement ranging from 10% to 75% reported in [29] for the links in an indoor environment. The average throughput they achieved for large packet size with frame aggregation is 80Mb/s for 40MHz channel and 64Mb/s for 20MHz channel, which are significantly lower than our findings. Our throughputs are close to the results in [23], where they achieved 113.2Mb/s without channel bonding and 197.8Mb/s with channel bonding using SDM mode for a lossless link in an indoor environment.

Our results indicate higher throughput gain from frame aggregation using wider channel and SGI. That means, if the data rate increases, the performance gain from frame aggregation will also be higher. On the other hand, we can not see significant improvement in throughput by increasing the channel width or reducing the guard interval when frame aggregation is disabled. This is because employing channel bonding and reducing the guard interval increase the physical data rate, but do not reduce the MAC layer overhead. This makes the overhead comparable to the packet transmission time. Thus to achieve higher throughput with the increment of PHY data rate of 802.11n, we need to enable frame aggregation. Similar observation is also made in [23].

2) Channel Width: To investigate the performance gain from channel bonding, we plot the throughput achieved in different MCS indices for different link lengths for both 20MHz and 40MHz channel widths with long guard interval in Figure 11. As we observed huge throughput improvement using frame aggregation, we only limit our current discussion with frame aggregation enabled. Figure 12 shows the maximum throughput achieved for each link length and channel width. We see that the throughput decreases with link length. On the other hand, we see at least 42% throughput gain from channel bonding. The improvement is greater for shorter links: 65% for the 300 m link and 58% for the 800 m link. It is interesting to see that the throughput gain gradually decreases with the increase in link lengths. Our observation is comparable to indoor environment results where 75% throughput gain is reported for channel bonding in [23] using SDM mode in a lossless link using frame aggregation, whereas improvement is achieved in the range of 33% to 100% in [29].

3) Short Guard Interval: To see how much throughput gain can be achieved using the Short Guard Interval, we plot the maximum throughput achieved for the 300 m link with frame aggregation enabled for different guard intervals for 40MHz channel width in Figure 13. We can see a mere 4.2% improvement in iperf throughput by using short guard interval. As SGI can increase PHY date rate by up to 11% [6], the 4.2% improvement in application layer throughput seems reasonable considering MAC and higher layer overheads.

4) Antenna Polarization Gain: To compare the gain of polarization diversity of the used MIMO antenna, we also measured the throughput in the 300m link using three 12 dBi omni-directional antenna, the same 5 GHz antenna we used in Section III, forming an antenna array at both ends of the link. We tested several different antenna placements such as linear array and triangle formation hoping to obtain enough path orthogonality to support two or more MIMO streams in a LOS environment. We also tested multiple spacings between the antenna elements from a few inches to 10 inches. In short, none of the tested antenna configurations provided orthogonality for two stream MCSs. Only MCSs 0 to 7 worked

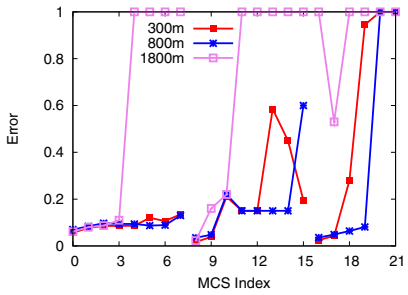

(a) 20MHz channel width

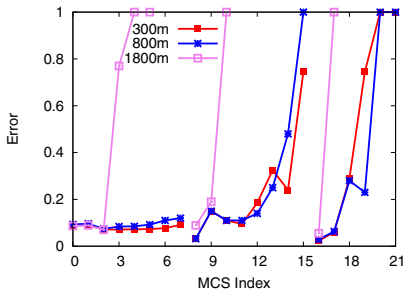

(b) 40 MHz channel width

Fig. 14. Error rate for different link lengths. Frame aggregation and long GI are used.

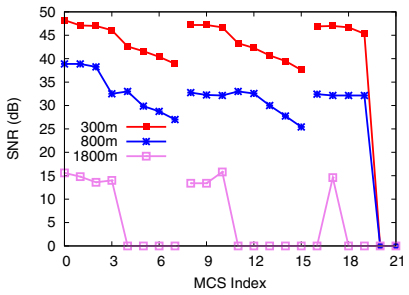

(a) 20MHz channel width

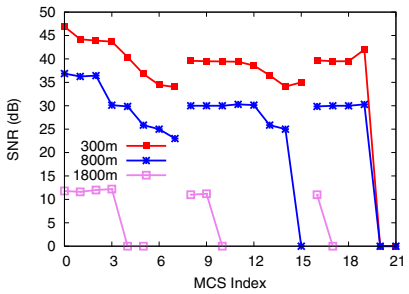

(b) 40 MHz channel width

Fig. 15. SNR for different link lengths. Frame aggregation and long GI are used.

with the non-polarization antenna array. According to the model in [16], at a frequency of 5 GHz, a maximum 50 meter distance is acceptable for 1 meter antenna spacing when the conventional linear placement is used.

Compared to the above result from non-polarization antenna, the MIMO antenna with differently polarized antenna elements clearly provides orthogonal path diversity for two stream MCSs and even for three stream MCSs with low modulation schemes as shown in Figure 9. Figure 11 shows the throughput of high rate MCSs of two and three streams begin to decrease as distance increases to 800 and 1800 meters.

To better understand the reasons why high rate MCSs do not work in longer distances, we plot error rate and SNR at each link length in Figures 14 and 15. Note that the error rates in Figure 14 are collected from the iperf server (receiver) reports and we set the iperf client transmission rate as the theoretical maximum achievable MAC throughput for given settings of MCS, channel width, guard interval, etc. MAC layer retransmissions, frame aggregation mechanism of the driver and iperf client transmission rate settings affect the iperf error rate and it does not exactly match the PHY layer error. Nevertheless high iperf error rate indicates severe packet losses in the physical layer. Here we see that the error rates inversely follow the throughput patterns shown in Figure 11.

As expected, the SNR in Figure 15 decreases with the increase in link length. Note that for a fixed number of streams, SNR decreases in higher MCS indices for each link length. This is because the sender transmits with lower power for the higher modulation schemes. The reason for this lower transmission power in higher MCS indices is to meet the EVM (Error Vector Magnitude) requirement, which is a design parameter to maintain the transmit quality. EVM is an indication how different imperfection in device implementation affects the transmit symbols [10]. The main contributors to EVM are compression and phase noise. For lower data rate, EVM is allowed to degrade which enables higher transmission power. For higher rates in 802.11n, EVM requirement is stricter. This may be one reason for low SNR for higher MCS rates. Another possible reason for the low SNR at the receiver in long links can be the Fresnel effect [3]. According to the Fresnel rule, 60% of the first Fresnel zone must be clear of obstacles. That means, to have a better signal strength at the receiver, any obstacle must not be closer to the 60% of the radius of the first Fresnel zone, measured from the direct line of sight link. Note that the radius of the Fresnel zone depends on the link length. Even in our case where the measurement is done on flat ground and the link has a direct line of sight with no major obstacles between the transmitter and the receiver, the ground itself besomes the obstacle. Using the equation in [3], we find that to nullify the Fresnel effect completely for a link length of 1800m, the antenna height should be at least 3.048m, where our antenna height is 3m. Here the curvature of the earth at the mid-point of the link is considered as obstacle.

Because of these reasons, the SNR at the receiver for higher MCS rates and longer links is low, which affects the error rate as the SNR is not strong enough for decoding. For example, we get the maximum throughput at MCS 15 for the 300 m link among the MCS rates with two streams (MCS $8 \sim 15$), whereas for the 800 m link we get the maximum at MCS 14. For the 300 m link, MCS 15 shows 38 dB SNR which is high enough to decode its modulation and coding (modulation type:64-QAM and coding rate=5/6). The SNR of MCS 15

for the 800 m link is 25.4 dB. Since the required SNR to decode 802.11a 54 Mb/s (64-QAM 3/4) is around 22 dB [19], MCS 15 (64-QAM 5/6) should require higher SNR to be decoded correctly. We see that 25.4 dB is not enough for MCS 15 (64-QAM 5/6). This indicates that the reason for packet losses in our experiments for different link lengths is low SNR, not the lack of diversity gain.

Moreover, we also see in Figure 11 that for most of the cases, the 300 m and the 800 m links perform similarly. But for these two link distances, three stream MCSs do not perform well. On the other hand, for the 1800 m link, we only get the connection for lower MCS rates for each number streams. These observations indicate that polarization gain of the antenna is in effect only up to the 800 m link in our experiments. Two stream MCS rates are supported by the polarization antenna for long range line-of-sight links, but three streams are limited and determined by SNR, and work well only with lower MCS rates with robust modulation and coding schemes.

V. Conclusion

We have considered an outdoor WiFi network for land-based oil and gas exploration wireless sensor networks. The scenario is different from the traditional long distance WiFi network in the sense that nodes are placed closer to ground level and long links also require high bandwidth.present a measurement experimental study of two types of links of this network. For the first-hop link, we use 802.11a/b/g to find the maximum link range and construct a path-loss model for our network. We use 802.11n for the backhaul link and evaluate different PHY/MAC layer features provided in 802.11n. We have shown that high throughput can be achieved in long distance links using 802.11n even in open spaced outdoor networks. We have obtained a maximum throughput of 148 Mb/s for the 800 m link and 40.8 Mb/s for the 1800 m link. We have also shown that two stream MCS rates are supported by the polarization antenna for long range line-of-sight links, but three streams work well only with low MCS rates. Our study can be complementary to the existing study on 802.11n as most of these analysis were done in indoor or urban environments.

Acknowledgment

We thank Jim Jackson at UC Davis Department of Plant Sciences for letting us use their land to perform our experiments. We are also grateful to John Balian, Rick Davis, Anil Gupta, Scott Lindsay, Vincent Ma, Hien Nguyen, and Tom Stefanski of HP Networking for their help.

References

[1] 2.4-2.5/5.1-5.9GHz Dual-Band MIMO Directional Antenna. http://www.lairdtech.com/WorkArea/DownloadAsset.aspx?id=3999.

[2] Atheros WLAN::AR9380. http://www.atheros.com/technology/technology.php?nav1=47&product=88.

[3] Fresnel Zone and Effect. http://www.zytrax.com/tech/wireless/fresnel.htm.

[4] HP E-M111 Client Bridge. http://h17007.www1.hp.com/us/en/products/wireless/HP_E-M111_Client_Bridge_Series/index.aspx.

[5] HP E-MSM422 Access Point. http://h30094.www3.hp.com/product.asp?sku=10256653&mfg_part=J9358B&pagemode=ca.

[6] IEEE 802.11n-2009Amendment 5: Enhancements for Higher Throughput. IEEE-SA. 29 October 2009.

[7] Iperf. http://dast.nlanr.net/projects/iperf.

[8] Laird Technologies 12 dBi omni-directional antenna for 2.4 GHz band. http://lairdtech.thomasnet.com/item/special-purpose-omnidirectional-antennas/omnidirectional-antennas/od24-12.

[9] Laird Technologies 12 dBi omni-directional antenna for 5.4-5.8 GHz band. http://lairdtech.thomasnet.com/item/special-purpose-omnidirectional-antennas/omnidirectional-antennas/od58-12.

[10] Practical Manufacturing Testing of 802.11 OFDM Wireless Devices. http://www2.litepoint.com/node/4984.

[11] Shell and HP dig for power. http://www.v3.co.uk/computing/features/2258362/shell-hp-dig-power.

[12] M. Y. Arslan, K. Pelechrinis, I. Broustis, S. V. Krishnamurthy, S. Addepalli, and K. Papagiannaki. Auto-configuration of 802.11n WLANs. In *Proc. CoNEXT*, 2010.

[13] P. Bhagwat, B. Raman, and D. Sanghi. Turning 802.11 inside-out. In *Proc. SIGCOMM*, 2004.

[14] K. Chebrolu, B. Raman, and S. Sen. Long-distance 802.11b links: Performance measurements and experience. In *Proc. MobiCom*, 2006.

[15] E. Gelal, K. Pelechrinis, S. Mohammed, A. Chockalingam, and S. Kasera. On the impact of MIMO diversity on higher layer performance. In *Proc. ICDCS*, 2010.

[16] D. Gesbert, H. Bolcskei, D. Gore, and A. Paulraj. Outdoor MIMO wireless channels: Models and performance prediction. *IEEE Transactions on Communication*, 50:1926–1934, 2002.

[17] P. Gupta, B. Jain, B. Raman, and P. Kulkarni. Link-level measurement of outdoor 802.11g links. In *Proc. WiMesh*, 2009.

[18] J. P. Kermoal, L. Schumacherl, F. Frederiksen, and P. E. Mogensen. Polarization Diversity in MIMO Radio Channels: Experimental Validation of a Stochastic Model and Performance Assessment. In *Proc. IEEE VTC*, 2001 Fall.

[19] J. Lee, J. Ryu, S.-J. Lee, and T. Kwon. Improved modeling of IEEE802.11a PHY through fine-grained measurements. *Computer Networks*, 54:641–657, 2010.

[20] A. Mainwaring, J. Polastre, R. Szewczyk, D. Culler, and J. Anderson. Wireless sensor networks for habitat monitoring. In *Proc. WSNA*, 2002.

[21] J. M. G. Pardo, M. Lienard, E. Simon, and P. Degauque. On the Possibility of Applying Polarization Diversity to MIMO Techniques in Tunnels. In *Proc. ACM MSWiM*, 2009.

[22] R. Patra, S. Nedevshi, S. Surana, and A. Sheth. WiLDNet: Design and implementation of high performance WiFi based long distance networks. In *Proc. NSDI*, 2007.

[23] K. Pelechrinis, T. Salonidis, H. Lundgren, and N. Vaidya. Analyzing 802.11n performance gains. In *MobiCom poster*, 2009.

[24] K. Pelechrinis, T. Salonidis, H. Lundgren, and N. Vaidya. Experimental characterization of 802.11n link quality at high rates. In *Proc. WiNTECH*, 2010.

[25] B. Raman and K. Chebrolu. Design and evaluation of a new MAC protocol for long distance 802.11 mesh networks. In *Proc. MobiCom*, 2005.

[26] T. S. Rappaport. *Wireless Communications: Principles and Practice*. IEEE Press, Piscataway, NJ, USA, 1996.

[27] I. Sarris and A. R. Nix. Design and performance assessment of high-capacity MIMO architectures in the presence of a line-of-sight component. *IEEE Transactions on Vehicular Technology*, 56, July 2007.

[28] A. Sheth, S. Nedevshi, R. Patra, and L. Subramanian. Packet loss characterization in WiFi-based long distance networks. In *Proc. Infocom*, 2007.

[29] V. Shrivastava, S. Rayanchu, J. Yoon, and S. Banerjee. 802.11n under the microscope. In *Proc. Internet Measurement Conference*, 2008.